THE JOURNAL OF PHYSICAL CHEMISTRY A LETTERS

2006, *110,* 9783−9787
Published on Web 07/22/2006

Dissolution of Oxygen Reduction Electrocatalysts in an Acidic Environment: Density Functional Theory Study

Zhihui Gu and Perla B. Balbuena*

Department of Chemical Engineering, Texas A&M University, College Station, Texas 77843

Received: June 3, 2006; In Final Form: July 6, 2006

Density functional theory is employed to determine the reaction thermodynamics of a group of chemical and electrochemical reactions chosen to investigate the dissolution of metal atoms from oxygen reduction reaction catalysts in an acid medium. Once a set of thermodynamically allowed reactions is established, those reactions are selected to investigate the relative stabilities of Pt atoms and of other transition metal atoms (Ir, Pd, Rh, Ni, and Co) toward the dissolution reactions. The dissolution reactions that are found thermodynamically favorable are electrochemical and involve adsorbed oxygenated compounds that are intermediate species of the oxygen reduction reaction. Iridium is found to be the most stable among the various pure metals in comparison to Pt. Most of the metals alloyed with Pt cause a decrease of the Pt stability against dissolution, except for Ni, which does not affect it. On the other hand, the influence of Pt on the stability of the second metal in the alloy follows the same trend as in pure metal catalysts, with Ir being the most stable. When both atoms in a PtM alloy are involved in dissolution reactions, alloyed Ir is also found more stable than Pt in a given dissolution reaction, and the same behavior is found in alloyed Co for most of the reactions studied.

1. Introduction

Carbon supported platinum or platinum-based alloy catalysts are commonly used as electrodes in polymer electrolyte membrane fuel cells (PEMFC) to catalyze the hydrogen oxidation on the anode and the oxygen reduction reaction (ORR) on the cathode side. The slower kinetics of the oxygen reduction reaction is one of the key points that needs to be addressed for improving the fuel cell operation efficiency.[1] Therefore, many research studies related to the analysis of the oxygen reduction reaction process catalyzed by platinum and platinum-based alloy surfaces have been reported.[2−7] In those studies the oxygen adsorption and dissociation process has been proposed as a series of proton and electron-transfer reactions, and the existence of oxygenated intermediates such as adsorbed O, OH, and OOH during the ORR process has been established. Platinum-based alloys have shown catalyzing activity similar to that of the pure platinum catalyst for the ORR,[8−10] and in some cases activities higher than those for pure Pt were suggested by experimental reports[11−13] in which Co, Ni, Cr, and Fe as the second metal species are commonly employed in Pt-based bimetallic cathode catalysts. It is interesting that these metals might not be the ones that cause the largest chemical perturbations on Pt when forming alloys.[14]

Durability of Pt or Pt-based alloy cathode catalysts in an acid environment during PEMFC operation is another challenge for long-term applications, as electrode active surface loss results in a substantial decrease of fuel cell performance.[15] It is reported that agglomeration of active Pt nanoparticles caused by dissolution of the smallest particles or active sites and subsequent sintering are one of the major reasons for the loss of active surface in phosphoric acid fuel cells.[16−18] For PEMFC, losses of electrocatalyst active surface were detected during operation due to metal catalyst cluster agglomeration and dissolution, which was confirmed by the presence of Pt and Cr (one of the alloy metals) in the cathode outlet water.[19] The precipitation of Pt in the electrolyte membrane close to the cathode and at the catalyst/membrane interface due to reduction of dissolved platinum species such as Pt^{2+} by permeating hydrogen[15,20] and the presence of Pt in water indicate that Pt dissolution plays an important role in active surface losses of PEMFC electrocatalysts.[15] Experimental reports on Pt and Pt-alloy cathode catalysts showed that Pd and Rh are more soluble than Pt in the same experimental conditions[21] and the metal dissolution rate of a Pt alloy with a PtM ratio of 3:1 is lower than that of a Pt alloy with PtM ratio of 1:1.[20]

In contrast to the extensive investigations reported about the ORR process on catalytic surfaces, a detailed analysis of the mechanisms behind the dissolution process of cathode catalysts has not been reported. Here we present a thermodynamic analysis of potential metal dissolution reactions in acid medium, using density functional theory (DFT) calculations to explore the relative stabilities of transition metals in relation to that of Pt. The study is performed by comparing the change in reaction Gibbs free energies for different metals in a given dissolution reaction.

2. Computational Details

Six transition metal atoms M (Co, Rh, Ir, Ni, Pd, Pt) from group VIIIA are used to model adsorption sites of oxygen reduction intermediates denoted as MO, MOH and MOOH. Dissolution reactions are listed in Scheme 1 and the rationale for their selection is introduced in the next section.

* Corresponding author. E-mail: balbuena@tamu.edu.

10.1021/jp063447o CCC: $33.50 © 2006 American Chemical Society

SCHEME 1: Possible Metal Dissolution Reactions

Reaction 1: $MOOH + 3H^+ + e^- \longrightarrow M^{2+} + 2H_2O$

Reaction 2: $MOH + MO + 3H^+ + e^- \longrightarrow M^{2+} + M + 2H_2O$

Reaction 3: $MOOH + MO + 5H^+ + e^- \longrightarrow 2M^{2+} + 3H_2O$

Reaction 4: $MOOH + MO + 5H^+ + 3e^- \longrightarrow M^{2+} + M + 3H_2O$

Reaction 5: $MOOH + MOH + 4H^+ + 2e^- \longrightarrow M^{2+} + M + 3H_2O$

Reaction 6: $MO + 2H^+ \longrightarrow M^{2+} + H_2O$

Reaction 7: $2MOH + 2H^+ \longrightarrow M^{2+} + M + 2H_2O$

Reaction 8: $MOOH + MOH + 4H^+ \longrightarrow 2M^{2+} + 3H_2O$

The solvated proton is modeled as $H_9O_4^+$ (four waters in the first hydration shell[22]) and the hydrated metal cations (M^{2+}) are modeled as $M(H_2O)_4^{2+}$ and $M(H_2O)_6^{2+}$ because divalent states and four-coordinate and six-coordinate complexes of transition metals are common.[23] The effect of the solvent beyond the first shell is not included, which could be a strong approximation to evaluate the absolute change of free energy of the reaction; however, such an effect is much less important in this study where we analyze relative free energy changes ($\Delta\Delta G$) with respect to the same reactions on pure Pt. In each electrochemical reaction, the electron energy is set to zero. The Gaussian03 Rev C.02 program package[24] was employed for all calculations. All geometries were fully optimized using B3LYP, which is the hybrid exchange functional Becke3[25] in combination with the LYP correlation functional,[26] with the LANL2DZ pseudopotential and double ξ basis set for transition metals[27] and with 6-311++g(d, p) for oxygen and hydrogen atoms. Frequency calculations were done for all optimized geometries at the same theoretical level as that of the geometry optimization to verify that the structures were global minima and to calculate the free energies. Different geometric, electronic and spin states were calculated for all species and only the ground states were used to calculate the free energy difference for the metal dissolution reactions.

Slab and small clusters usually are used to model metal surfaces for studying oxygen adsorption and reduction reactions using DFT calculations, providing reasonable results.[7,28−32] For the cathode catalyst dissolution process, our investigation starts analyzing reactions that involve oxygen reduction intermediates adsorbed on a metal M (MO, MOH, MOOH), where M is represented by a single atom or by a dimer. Comparison of the ΔG for each possible dissolution reaction provides the thermodynamic relative stabilities of metal catalysts against dissolution, though the single atom and the dimer models are approximations to the catalytic site. As shown in Scheme 1, the reactions involve the adsorption of O and OH species to the pure metal or metal alloys. Thus, it is crucial for the model to be able to accurately describe the binding energies of these species to a metal atom or to a dimer. In fact, such small metal clusters have proven useful to understand the mechanism of the oxygen reduction reaction, where determining binding energies of intermediate species such as O and OH are of the utmost importance.[6,7,33] In addition, we focus on free energy differences of metal dissolution reactions, which could cancel the errors arising from the approximate metal model to some extent and can provide valuable predictions.

The ΔG for each dissolution reaction is calculated as the difference between free energies of products and reactants, for example, reaction 2 in Scheme 1 for a single metal atom M and for a metal dimer MM model with the hydrated metal cation modeled as $M(H_2O)_6^{2+}$ are written as (1) and (2) respectively:

$$\Delta G = G[M(H_2O)_6^{2+}] + G[M] + 3G[(H_2O)_4] + 2G[H_2O] - G[MOH] - G[MO] - 3G[H_9O_4^+] - G[(H_2O)_6] \quad (1)$$

$$\Delta G = G[M(H_2O)_6^{2+}] + G[M] + G[MM] + 3G[(H_2O)_4] + 2G[H_2O] - G[MMOH] - G[MMO] - 3G[H_9O_4^+] - G[(H_2O)_6] \quad (2)$$

3. Results and Discussion

3.1. Thermodynamic Analysis of Pt Dissolution. The possible metal dissolution reactions from oxygen reduction intermediates of MO, MOH and MOOH proposed in Scheme 1 include both chemical and electrochemical dissolution reactions. In reactions 1, 6, and 7, the oxygen reduction intermediates interact with a proton to produce metal cations, and in reactions 2−5 and in reaction 8 *adjacent* oxygen reduction intermediates adsorbed on the catalyst surface interact with each other and with a proton to produce metal cations and water. The calculated Gibbs free energy changes of reaction 1 to reaction 8 are listed in Table 1. The difference between the ΔG of a given dissolution reaction in Table 1 is due to the variation in the hydration energies of the cation with different water coordination number, and to the metal bond dissociation energy involved in the dimer model. The ΔG's of reactions 6−8 are positive whereas the ΔG's of the other reactions are negative (except for Pt dimer in reaction 3, $Pt(H_2O)_4^{2+}$ model), indicating that all of the dissolution reactions are thermodynamically favorable except for reactions 6−8 with the $Pt(H_2O)_6^{2+}$ model. From Scheme 1, the thermodynamically favorable dissolution reactions are electrochemical, whereas, the chemical dissolution reactions 6−8 are thermodynamically unfavorable. Among the thermodynamically favorable dissolution reactions, reaction 4 has the highest negative ΔG, which indicates that the more electrons involved, the higher the equilibrium constant of the associated reaction. The conclusions arising from this initial set of calculations are that the possible Pt cathode catalyst dissolution reactions (reactions 1−5 in Scheme 1) are electrochemical, and that all the oxygen reduction intermediates can be involved in the dissolution reactions. We have discussed in the "Computational Details" section that the main two approximations of this study are neglecting the "bulk" solvent effect beyond the first shell and using a single atom or a dimer to represent the catalytic site, and we argued that such approximations should not affect the conclusions related to the *relative* changes of reaction free energy. A valid question may be how these approximations may affect the absolute ΔG's. Thus, we observe that once the full solvation effects for metal cation complexes are taken into account, more negative free energies for metal cations should be obtained. Besides, on the basis of the magnitude of the ΔG's in Table 1, we estimate that the clear distinction shown between reactions 1−5 and reactions 6−8 makes it unlikely that the conclusions given in this section may be reverted by the use of a more elaborate model. The elementary reactions and corresponding mechanism for each thermodynamically favorable dissolution reaction will be investigated in future work.

3.2. Thermodynamic Analysis of the Stability against Dissolution of Metals Other Than Pt. During the cathode catalyst dissolution process, metal−metal bond dissociation processes are involved, which are followed by cation hydration. Therefore, at least two metal atoms should be included in the cathode catalyst model. However, initially, we compute the single metal atom relative dissolution stability as the simplest

TABLE 1: Gibbs Free Energy Changes (ΔG, in eV) Calculated with B3LYP/LANL2DZ and 6-311++G(d,p) of Possible Pt Dissolution Reactions Listed in Scheme 1, Modeling the Hydrated Cation as $Pt^{2+}(H_2O)_4$ and as $Pt^{2+}(H_2O)_6$

reactions	ΔG^a	ΔG^b	ΔG^c	ΔG^d
1	−6.26	−7.12	−4.14	−5.00
2	−4.02	−4.88	−2.82	−3.68
3	−3.54	−5.25	0.05	−1.66
4	−20.59	−21.44	−19.32	−20.17
5	−13.01	−13.87	−11.18	−12.04
6	2.72	1.88	4.20	3.34
7	3.55	2.69	5.30	4.45
8	4.04	2.32	5.87	4.16

[a] Pt^{2+} modeled as $Pt^{2+}(H_2O)_4$ and single metal atom model. [b] Pt^{2+} modeled as $Pt^{2+}(H_2O)_6$ and single metal atom model. [c] Pt^{2+} modeled as $Pt^{2+}(H_2O)_4$ and metal dimer model. [d] Pt^{2+} modeled as $Pt^{2+}(H_2O)_6$ and metal dimer model.

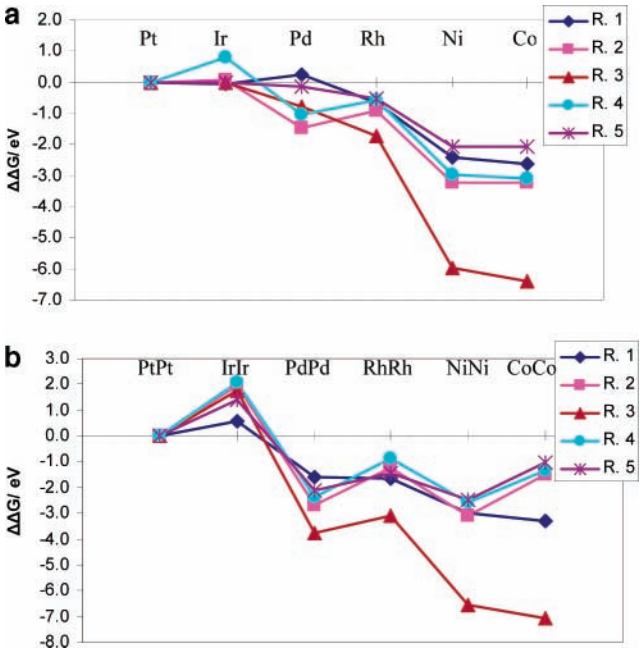

Figure 1. (a) $\Delta\Delta G$ (eV) of possible dissolution reactions of Pt, Pd, Ni, Ir, Rh, and Co (single atom model) based on $M(H_2O)_6^{2+}$ calculated with B3LYP/LANL2DZ and 6-311++g(d,p). (b) $\Delta\Delta G$ (eV) of possible dissolution reactions of Pt, Pd, Ni, Ir, Rh, and Co (dimer model) based on $M(H_2O)_6^{2+}$ with B3LYP/LANL2DZ and 6-311++g(d,p).

catalyst model, and we compare the results with those of a dimer model of dissolution. The other five metals (Co, Rh, Ir, Ni, Pd) besides Pt were studied on the basis of the five thermodynamically favorable dissolution reactions. The calculated ΔG's for these metals (using single atom and metal dimer models) for dissolution reactions 1−5 (Scheme 1) are negative (except for some dimer cases in reaction 3; data available as Supporting Information) on the basis of $M(H_2O)_4^{2+}$ and $M(H_2O)_6^{2+}$, respectively, which indicates that the dissolution reactions for almost all these metals are also thermodynamically favorable. The ΔG of reaction 4 in which the highest number of electrons is involved has the highest negative value for all the studied metals. Figure 1a shows the relative stability of each of the metal atoms relative to Pt for each dissolution reaction based on $\Delta\Delta G$, which is defined as

$$\Delta\Delta G = \Delta G_M - \Delta G_{Pt} \qquad M = Ir, Pd, Rh, Ni, Co$$

Negative $\Delta\Delta G$ means that the corresponding metal is more unstable than the Pt atom in the given dissolution reaction in an acid medium. For each reaction, Co and Ni are the metals that are more easily dissolved than the other four metals from the point of view of thermodynamics, with ΔG's significantly more negative (>2.0 eV) than that of the Pt atom, especially in reaction 3, whereas Pt and Ir are the most stable metals according to this criterion (Figure 1a). The stability of Ir is very similar to that for Pt in all reactions except reaction 4, in which Ir is more stable with a $\Delta\Delta G$ value of ∼0.8 eV. Generally, Pd is more unstable compared with the Pt atom and the range of variation of $\Delta\Delta G$ for the five dissolution reactions in this case is +0.2 to −1.4 eV. Rh is also more unstable compared with Pt and the $\Delta\Delta G$ values converge around −0.7 eV except for reaction 3. In summary, using the single atom model, the dissolution stability sequence is Co < Rh < Ir in the ninth column and Ni < Pd < Pt in the tenth column (group VIIIA) of the periodic table.

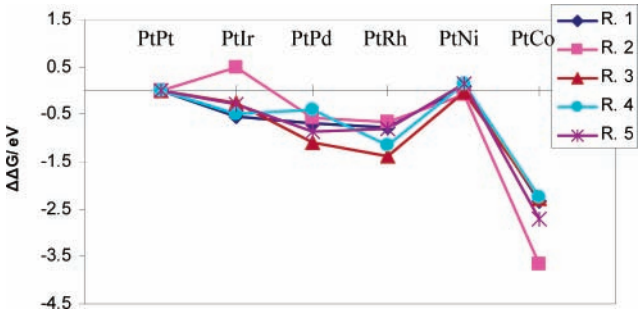

Figure 2. $\Delta\Delta G$ (eV) of Pt dissolution reactions in PtPt, PtPd, PtNi, PtIr, PtRh, and PtCo alloy cathode catalysts based on $M(H_2O)_6^{2+}$ with B3LYP/LANL2DZ and 6-311++g(d,p).

Figure 1b shows the relative stabilities of metal catalysts based on the dimer catalyst model in which the metal bond dissociation is included, and consequently, we expect the results to be more realistic than those of the single atom catalyst model. Different from the single atom model, Ir is more stable than Pt catalyst with positive $\Delta\Delta G$'s for all dissolution reactions, due to the higher dissociation energy of 2.85 eV of the Ir dimer compared to 2.32 eV dissociation energy of the Pt dimer. Similarly to the single atom model results, Pd and Rh are more unstable than Pt for the electrochemical dissolution reactions. In contrast to the single atom model, Rh shows slightly improved stability than Pd in all five dissolution reactions. In the single atom model, Co and Ni have similar stabilities relative to Pt (Figure 1a), whereas Figure 1b shows that the Co catalyst is more stable than the Ni cathode catalyst in most of the dissolution reactions, including the metal bond dissociation. Figure 1b also shows that the Ni catalyst is the most unstable among the six types of metal cathode catalysts. In summary, because the stability of the cathode catalysts against dissolution depends on the combined effects of all dissolution reactions, an approximate relative stability order from Figure 1b is Ir > Pt > Rh > Pd > Co > Ni based on the average values of $\Delta\Delta G$ (1.55, 0, −1.65, −2.50, −2.85, and −3.53 eV, respectively).

3.3. Pt Stability against Dissolution in Pt-Based Bimetallic Alloy Cathode Catalysts. Pt−M alloys were studied on the basis of the thermodynamically stable five dissolution reactions (Scheme 1) to investigate the effects of the introduction of a second metal on the Pt stability against dissolution compared with that of pure Pt. Alloy cathode catalysts with Pt:M ratio of 1: 1 are modeled as Pt-M dimer and the O, OH, and OOH adsorbents assumed to *bind to Pt sites*. Figure 2 shows the relative Pt site stabilities of five types of cathode alloy catalysts compared with that of pure Pt based on the dissolution reactions for which $\Delta\Delta G$ is defined as

$$\Delta\Delta G = \Delta G_{PtM} - \Delta G_{PtPt} \qquad M = Ir, Pd, Rh, Ni, Co$$

Negative $\Delta\Delta G$ means that Pt in the corresponding alloy is more unstable than pure Pt for a given dissolution reaction in acid medium. Figure 2 shows that pure Pt is more stable than Pt in other five alloy catalysts and the presence of a second metal species decreases the stability of Pt adsorption sites. Introduction of Ir, Pd, and Rh decreases the Pt stability in alloy catalysts of PtIr, PtPd and PtRh more than that it does Ni in PtNi. Pt in PtNi almost has stability similar to that of the pure Pt cathode catalyst, whereas Pt in PtCo alloy is the most unstable cathode catalyst of this group. Our calculation results showing that the 1:1 PtNi alloy cathode catalyst is more stable than the 1:1 PtCo alloy cathode are consistent with the experimental report in which PtNi/C cathode alloy catalysts showed dissolution rates lower than those of PtCo/C alloy catalysts.[20] From Figure 2, Ni is the best metal to be alloyed with the Pt catalyst without decreasing the Pt stability against dissolution; obviously this criterion does not refer to optimizing the catalyst in terms of oxygen reduction activity, which follows different rules as discussed in previous work.[32]

3.4. Alloyed Metal Stability against Dissolution in Pt-Based Bimetallic Alloy Cathode Catalysts. In the previous section we discussed the Pt relative stabilities in alloy catalysts compared with that of Pt in a pure Pt cathode catalyst. In an alloy, it is also important to determine the relative stabilities of the second metal M species. Here the *adsorption sites are M sites* to which the O, OH, and OOH are assumed to bind instead of binding to Pt, with the $\Delta\Delta G$ defined as

$$\Delta\Delta G = \Delta G_{PtM} - \Delta G_{PtPt} \qquad M = Pt, Ir, Pd, Rh, Ni, Co$$

The values of $\Delta\Delta G$ shown in Figure 3 indicate that all dissolution reactions show very similar trends of relative dissolution stabilities as those in Figure 1b for the respective pure metals. Ni and Co show much lower stability in reaction 3 than other metal species. Ir is the most stable metal in the Pt-based bimetallic alloy compared with the other four metals (Pd, Rh, Ni, Co) in PtM alloys and even more stable than Pt in the pure Pt cathode catalyst. Approximately, Pd, Ni, and Co have similar stabilities in the dissolution reactions except for reaction 3, for which Ni and Co having similar stabilities are the most unstable, and Pd and Rh behave similarly to each other and are more stable that Ni and Co, but still strongly unstable with respect to Pt and Ir. Thus, the similarity between Figure 1b and Figure 3 indicates that the relative stabilities of second metals in Pt-based bimetallic alloys correlate well with the stabilities of the corresponding pure metal cathode catalysts in the same acidic environment.

3.5. Comparison of Pt and M Stabilities against Dissolution in the Same Pt-Based Bimetallic PtM Alloy. The results shown in Figure 4 are based on the values of $\Delta\Delta G$, defined as $\Delta\Delta G = \Delta G_1 - \Delta G_2$, where ΔG_1 is the free energy for the second species M as adsorption site in each dissolution reaction for a PtM alloy, and ΔG_2 is the free energy for Pt as adsorption site in PtM in each dissolution reaction. Therefore, the negative $\Delta\Delta G$ indicates that the Pt site is more stable than those of the second metal species in Pt-based bimetallic cathode catalysts assuming that *both* Pt and the other metal species are able to act as adsorption sites for O, OH, and OOH. Certainly the $\Delta\Delta G$'s are zero for PtM = PtPt. Figure 4 shows that Ir is more stable than Pt in the PtIr alloy cathode catalyst due to the positive $\Delta\Delta G$ values in all five dissolution reactions. The metal Co is also more stable than or equally stable to Pt in the PtCo alloy except in reaction 3. Pd, Rh, and Ni are less stable than Pt in

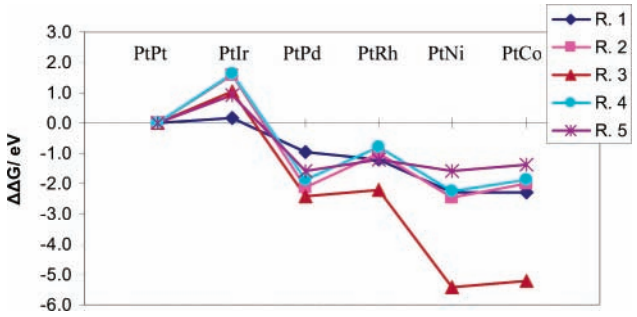

Figure 3. $\Delta\Delta G$ (eV) of dissolution reactions of metal Pt, Pd, Ni, Ir, Rh, and Co in PtPt, PtPd, PtNi, PtIr, PtRh, and PtCo alloy cathode catalyst based on $M(H_2O)_6^{2+}$ with B3LYP/LANL2DZ and 6-311++g-(d,p).

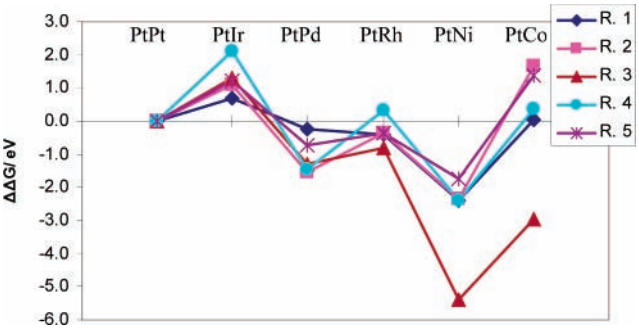

Figure 4. $\Delta\Delta G$ (eV) of dissolution reactions of metal Pt vs Pt, Pd, Ni, Ir, Rh, and Co in PtPt, PtPd, PtNi, PtIr, PtRh, and PtCo alloy cathode catalyst based on $M(H_2O)_6^{2+}$ with B3LYP/Lanl2dz and 6-311++g-(d,p).

PtPd, PtRh and PtNi alloy cathode catalysts, respectively, which is consistent with the experimental report that Pd and Rh are more soluble than Pt in an acid environment.[21]

4. Conclusions

Analyses of the calculated ΔG's of possible dissolution reactions involving adsorbed oxygen reduction intermediates indicate that five dissolution reactions of oxygen reduction reaction catalysts are thermodynamically favorable. These cathode catalyst dissolution reactions are electrochemical instead of chemical reactions, and the magnitude of the negative ΔG increases with the number of electrons involved in the process. The relative stabilities against dissolution of different pure metal cathode catalysts (Pt, Ir, Pd, Rh, Ni, Co) with respect to Pt based on the $\Delta\Delta G$ for each dissolution reaction indicate that Ir is the most stable pure catalyst.

For alloy cathode catalysts, the introduction of a second metal influences the Pt stability in the alloy catalysts, except for Ni which has little influence on the Pt stability in a PtNi alloy compared with the stability of Pt in pure Pt catalyst. The presence of Ir, Pd, Rh, and Co decreases the stability of Pt in PtIr, PtPd, PtRh and PtCo, respectively, compared with Pt in a pure Pt cathode catalyst.

The relative stabilities of Ir, Pd, Rh, Ni, Co in the corresponding alloy cathode catalysts show trends similar to those of the corresponding pure cathode catalysts, Ir (in Pt−Ir) being the most stable. Comparing the relative stabilities to a given dissolution reaction of Pt and another metal species in the same alloy cathode catalyst, it is found that Ir and Co are more stable than Pt in PtIr and PtCo, respectively.

Acknowledgment. This work was supported by the Department of Energy, grant DE-FG02-05ER15729. This research used

resources of the National Energy Research Scientific Computing Center, which is supported by the Office of Science of the U.S. Department of Energy under Contract No. DE-AC03-76SF00098.

Supporting Information Available: Tables of Gibbs energies. This material is available free of charge via the Internet at http://pubs.acs.org.

References and Notes

(1) Gasteiger, H. A.; Kocha, S. S.; Sompalli, B.; Wagner, F. T. Activity benchmarks and requirements for Pt, Pt-alloy, and non-Pt oxygen reduction catalysts for PEMFCs. *Appl. Catal. B: Environ.* **2005**, *56*, 9−35.

(2) Wang, Y.; Balbuena, P. B. Ab initio Molecular Dynamics Simulations of the Oxygen Electroreduction Reaction on a Pt(111) Surface in the Presence of Hydrated Hydronium $(H_3O)+(H_2O)_2$: Direct or Series Pathway? *J. Phys. Chem. B* **2005**, *109*, 14896−14907.

(3) Xu, Y.; Ruban, A. V.; Mavrikakis, M. Adsorption and dissociation of O_2 on Pt−Co and Pt−Fe alloys. *J. Am. Chem. Soc.* **2004**, *126*, 4717−4725.

(4) Murthi, V. S.; Urian, R. C.; Mukerjee, S. Oxygen reduction kinetics in low and medium-temperature acid environment: Correlation of water activation and surface properties in supported Pt and Pt alloy electrocatalysts. *J. Phys. Chem. B* **2004**, *108*, 11011−11023.

(5) Sidik, R. A.; Anderson, A. B. Density functional theory study of O_2 electroduction when bonded to a Pt dual site. *J. Electroanal. Chem.* **2002**, *528*, 69−76.

(6) Anderson, A. B.; Albu, T. V. Catalytic effect of platinum on oxygen reduction: An ab initio model including electrode potential dependence. *J. Electrochem. Soc.* **2000**, *147*, 4229−4238.

(7) Panchenko, A.; Koper, M. T. M.; Shubina, T. E.; Mitchell, S. J.; Roduner, E. Ab Initio Calculations of Intermediates of Oxygen Reduction on Low-Index Platinum Surfaces. *J. Electrochem. Soc.* **2004**, *151*, A2016-A2027.

(8) Markovic, N. M.; Ross, P. N. Surface Science Studies of Model Fuel Cells Electrocatalysts. *Surf. Sci. Rep.* **2002**, *45*, 117−229.

(9) Mukerjee, S.; Srinivasan, S.; Soriaga, M. P. Effect of Preparation Conditions of Pt Alloys on Their Electronic, Structural, and Electrocatalytic Activities for Oxygen Reduction-XRD, XAS, and Electrochemical Studies. *J. Phys. Chem.* **1995**, *99*, 4577−4589.

(10) Yu, P.; Pemberton, M.; Plasse, P. PtCo/C cathode catalyst for improved durability in PEMFCs. *J. Power Source* **2004**, *144*, 11−20.

(11) Paulus, U. A.; Vokaun, A.; Scherer, G. G.; Schmidt, T. J.; Stamenkovic, V.; Radmilovic, V.; Markovic, N. M.; Ross, P. N. Oxygen reduction on carbon-supported Pt−Ni and Pt−Co alloy catalysts. *J. Phys. Chem. B* **2002**, *106*, 4181−4191.

(12) Paulus, U. A.; Vokaun, A.; Scherer, G. G.; Schmidt, T. J.; Stamenkovic, V.; Markovic, N. M.; Ross, P. N. Oxygen reduction on high surface area Pt-based alloy catalysts in comparison to well-defined smooth bulk alloy electrodes. *Electrochim. Acta* **2002**, *47*, 3787−3798.

(13) Mukerjee, S.; Srinivasan, S. Enhanced electrocatalysis of oxygen reduction on platinum alloys in proton-exchange membrane fuel cells. *J. Electroanal. Chem.* **1993**, *357*, 201−224.

(14) Rodriguez, J. A. Physical and chemical properties of bimetallic surfaces. *Surf. Sci. Rep.* **1996**, *24*, 223−287.

(15) Ferreira, P. J.; la O, G. J.; Shao-Horn, Y.; Morgan, D.; Makharia, R.; Kocha, S. S.; Gasteiger, H. A. Instability of Pt/C Electrocatalysts in Proton Exchange Membrane Fuel Cells. *J. Electrochem. Soc.* **2005**, *152*, A2256-A2271.

(16) Roh, W.; Cho, J.; Kim, H. Characterization of Pt−Cu−Fe ternary electrocatalysts supported on carbon black. *J. Appl. Electrochem.* **1996**, *26*, 623−630.

(17) Kim, K. T.; Kim, Y. G.; Chung, J. S. Effect of surface roughening on the catalytic activity of Pt−Cr electrocatalysts for the oxygen reduction in phosphoric acid fuel cell. *J. Electrochem. Soc.* **1995**, *142*, 1531−1538.

(18) Honji, A.; Mori, T.; Tamura, K.; Hishinuma, Y. *J. Electrochem Soc.* **1988**, *135*, 355−359.

(19) Xie, J.; Wood, D. L., III; Wayne, D. M.; Zawodzinski, T. A.; Atanassov, P.; Borup, R. L. Durability of PEFCs at High Humidity Conditions. *J. Electrochem. Soc.* **2005**, *152*, A104-A113.

(20) Colon-Mercado, H. R.; Popov, B. N. Stability of platinum based alloy cathode catalysts in PEM fuel cells. *J. Power Source* **2005**, *155*, 253−263.

(21) Lukaszewski, M.; Czerwinski, A. Dissolution of noble metals and their alloys studied by electrochemical quartz crystal microbalance. *J. Electroanal. Chem.* **2006**, *589*, 38−45.

(22) Tawa, G. J.; Topol, I. A.; Burt, S. K.; Caldwell, R. A.; Rashin, A. A. Calculation of the aqueous solvation free energy of the proton. *J. Chem. Phys.* **1998**, *109*, 4852−4863.

(23) Cotton, A. F.; Wilinson, G.; Murillo, C. A.; Bochmann, M. *Advanced Inorganic Chemistry*, 6th ed.; Wiley: New York, 1999.

(24) Frisch, M. J.; Trucks, G. W.; Schlegel, H. B.; Scuseria, G. E.; Robb, M. A.; Cheeseman, J. R.; Montgomery, J. A.; Vreven, T.; Kudin, K. N.; Burant, J. C.; Millam, J. M.; Iyengar, S. S.; Tomasi, J.; Barone, V.; Mennucci, B.; Cossi, M.; Scalmani, G.; Rega, N.; Petersson, G. A.; Nakatsuji, H.; Hada, M.; Ehara, M.; Toyota, K.; Fukuda, R.; Hasegawa, J.; Ishida, M.; Nakajima, T.; Honda, Y.; Kitao, O.; Nakai, H.; Klene, M.; Li, X.; Knox, J. E.; Hratchian, H. P.; Cross, J. B.; Bakken, V.; Adamo, C.; Jaramillo, J.; Gomperts, R.; Stratmann, R. E.; Yazyev, O.; Austin, A. J.; Cammi, R.; Pomelli, C.; Ochterski, J. W.; Ayala, P. Y.; Morokuma, K.; Voth, G. A.; Salvador, P.; Dannenberg, J. J.; Zakrzewski, V. G.; Dapprich, S.; Daniels, A. D.; Strain, M. C.; Farkas, O.; Malick, D. K.; Rabuck, A. D.; Raghavachari, K.; Foresman, J. B.; Ortiz, J. V.; Cui, Q.; Baboul, A. G.; Clifford, S.; Cioslowski, J.; Stefanov, B. B.; Liu, G.; Liashenko, A.; Piskorz, P.; Komaromi, I.; Martin, R. L.; Fox, D. J.; Keith, T.; Al-Laham, M. A.; Peng, C. Y.; Nanayakkara, A.; Challacombe, M.; Gill, P. M. W.; Johnson, B.; Chen, W.; Wong, M. W.; Gonzalez, C.; Pople, J. A. *Gaussian03*, revision C.02 ed.; Gaussian, Inc.: Wallingford, CT, 2004.

(25) Becke, A. D. Density-functional thermochemistry. III. The role of exact exchange. *J. Chem. Phys.* **1993**, *98*, 5648−5652.

(26) Lee, C.; Yang, W.; Parr, R. G. Development of the Colle-Salvetti correlation-energy formula into a functional of the electron density. *Phys. Rev. B* **1988**, *37*, 785−789.

(27) Wadt, W. R.; Hay, P. J. Ab initio effective core potentials for molecular calculations. Potentials for main group elements Na to Bi. *J. Chem. Phys.* **1985**, *82*, 284−298.

(28) Balbuena, P. B.; Altomare, D.; Vadlamani, N.; Bingi, S.; Agapito, L. A.; Seminario, J. M. Adsorption of O, OH, and H_2O on Pt-based bimetallic clusters alloyed with Co, Cr, and Ni. *J. Phys. Chem. A* **2004**, *108*, 6378−6384.

(29) Norskov, J. K.; Rossmeisl, J.; Logadottir, A.; Lindqvist, L.; Kitchin, J. R.; Bligaard, T.; Jonsson, H. Origin of the overpotential for oxygen reduction at a fuel-cell cathode. *J. Phys. Chem. B* **2004**, *108*, 17886−17892.

(30) Jacob, T.; Muller, R. P.; W. A. Goddard, I. Chemisorption of Atomic Oxygen on Pt(111) from DFT Studies of Pt−Clusters. *J. Phys. Chem. B* **2003**, *107*, 9465−9476.

(31) Li, T.; Balbuena, P. B. Computational studies of the interactions of oxygen with platinum clusters. *J. Phys. Chem. B* **2001**, *105*, 9943−9952.

(32) Wang, Y.; Balbuena, P. B. Design of oxygen reduction bimetallic catalysts: Ab initio derived thermodynamic guidelines. *J. Phys. Chem. B* **2005**, *109*, 18902−18906.

(33) Anderson, A. B.; Albu, T. V. Ab initio determination of reversible potentials and activation energies for outer-sphere oxygen reduction to water and the reverse oxidation reaction. *J. Am. Chem. Soc.* **1999**, *121*, 11855−11863.